Appl. Phys. 8, 333—340 (1975)

Applied Physics

Infrared Stimulated Raman Generation: Effects of Gain Focussing on Threshold and Tuning Behaviour

D. Cotter, D. C. Hanna and *R. Wyatt*

Department of Electronics, University of Southampton, Southampton, U.K.

Received 7 July 1975/Accepted 4 August 1975

Abstract. It is shown that for generation of infrared radiation by stimulated Raman scattering, the diffraction spread of the Stokes wave can have a significant effect on the threshold. Compared with an analysis in which gain focussing is neglected, the threshold powers may be much higher with a corresponding reduction in tuning range. The design of a Raman oscillator is considerably influenced by these diffraction effects, and also it is found that the Stokes wave is subject to frequency-pulling which is dependent on the pump power.

Index Headings: Tunable lasers — Infrared — Stimulated Raman effect — Gain focussing

It has been demonstrated recently that stimulated Raman scattering in gases [1, 2] and atomic vapours [3–8] provides an efficient method of generating tunable infrared radiation. The simplicity of the technique makes it attractive for infrared spectroscopy [7], and it is interesting therefore to examine the possibilities of extending the tuning to longer wavelengths.

The large frequency shifts (20000–30000 cm^{-1}) available from electronic Raman transitions in atomic vapours can in principle allow wide ranges of infrared tuning for the Stokes wave, using currently available dye lasers as the pump source. High efficiencies are possible when the pump frequency is close to resonance with a real intermediate level (resonance Raman scattering). The frequency dependence of the Raman gain coefficient G is given by [7]

$$G \propto \omega_s/[\omega_{fi}(\Delta\omega)^2]\,, \tag{1}$$

where ω_s is the Stokes frequency, $\Delta\omega$ is the detuning of the pump frequency from the real intermediate level i, and ω_{fi} is the frequency of the transition between the final Raman state f and level i (see Fig. 1). Since the gain coefficient is inversely proportional to $(\Delta\omega)^2$, it is necessary to choose a system with closely spaced intermediate and final energy levels in order to produce tunable radiation

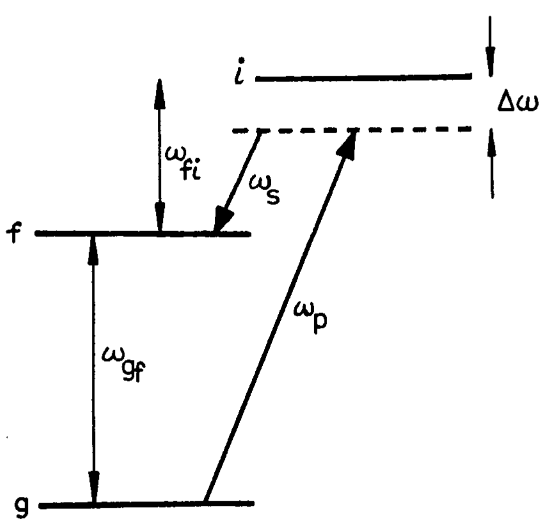

Fig. 1. Energy level diagram

at longer infrared wavelengths. The inverse square law dependence also means that, for a given pump power, an increase in the Raman threshold will decrease the available tuning range. Two factors tend to raise the threshold for long wavelength generation. Firstly, the gain coefficient is proportional to the Stokes frequency. Secondly, as the ratio of the pump and Stokes wavelengths becomes small, the diffraction loss of the Stokes light increases. This diffraction loss can be large since the pump radiation will usually be focussed to a narrow beam in the Raman medium. Only the Stokes radiation which remains inside the narrow pumped region is amplified and is therefore observed emerging as a collimated beam having dimensions similar to that of the pump. It is this effect which is termed gain focussing, and this paper analyses the effects of gain focussing on the behaviour of infrared stimulated Raman scattering.

The approach taken here is to use the theory of gain focussing first formulated by Kogelnik [9], and which has been successful in describing the performance of certain types of high gain laser [10–16]. Following a similar analysis, we are able to describe the growth of Raman scattered radiation within the paraxial-ray limits of Gaussian beam theory. A small signal analysis will be developed in which depletion of the pump beam and saturation of the medium are neglected, and it therefore cannot be used to describe the detailed behaviour of the generated beams when operating well into saturation. However the theory can be used to analyse the threshold behaviour from which calculations of the expected tuning range can be made, and the results have important implications for the design of infrared Raman devices.

1. Gain Focussing Theory of Raman Scattering

We begin by seeking solutions for the wave equation which describes the propagation of the generated radiation. A uniform Raman active medium is pumped by a laser beam travelling in the z direction, and the wave equation (in MKSA units) for the resulting stimulated radiation at the Stokes frequency ω_s is

$$\nabla_T^2 E(\omega_s) + \partial^2 E(\omega_s)/\partial z^2 + k_s^2 E(\omega_s) + \mu_0 \omega_s^2 P(\omega_s) = 0 \quad (2)$$

where ∇_T^2 is the transverse component of the Laplace operator ∇^2. The Stokes field is related to the complex Fourier amplitude $E(\omega_s)$ by

$$E_s(t) = \tfrac{1}{2}\left[E(\omega_s)\exp(j\omega_s t) + \mathrm{cc}\right] \quad (3)$$

and there is a corresponding equation with subscript p denoting the pump field. The nonlinear Stokes polarisation is defined in terms of the Raman susceptibility as

$$P(\omega_s) = \varepsilon_0 \chi^{(3)}(-\omega_s;\, \omega_p,\, -\omega_p,\, \omega_s)\; E(\omega_p)\, E(\omega_p)^* E(\omega_s)\,. \quad (4)$$

At first we will consider the case where the pump and Stokes frequencies are in exact resonance with the Raman transition,

$$\omega_s = \omega_p - \omega_{gf}\,. \quad (5)$$

The nonlinear susceptibility is then purely imaginary [17], and may be written

$$\chi^{(3)}(-\omega_s;\, \omega_p,\, -\omega_p,\, \omega_s) = j\,\chi_R \quad (6)$$

with χ_R real.

For solutions propagating mainly in the z direction we will substitute

$$E(\omega_{s,p}) = E_{s,p} \exp(-jk_{s,p} z) \quad (7)$$

where k_s and k_p are the real propagation constants for the Stokes and pump waves, respectively. (In fact, the following small signal theory can be applied equally to both forward and backward travelling waves.) The result of substituting for $E(\omega_s)$ in (2), and making the usual paraxial approximations [18], is

$$\nabla_T^2 E_s - 2jk_s \partial E_s/\partial z + jk_s G E_s = 0 \quad (8)$$

where

$$G = \omega_s^2 \chi_R E_p E_p^* / k_s c^2\,. \quad (9)$$

Here, G is the plane wave power gain coefficient which is sometimes written as gI_p where I_p is the incident pump intensity [7]. Since the pump field varies over the beam cross-section (transverse to the direction of propagation z), then through (9) there is a corresponding variation in the Raman gain profile which gives rise to focussing and guiding of the Stokes light [19]. No straightforward analytical solutions for (8) exist for the most interesting practical situation in which the incident laser beam has a Gaussian radial field distribution,

$$|E_p| = |E_{po}| \exp(-r^2/W_p^2)\,. \quad (10)$$

In this case, it follows from (9) that

$$G = G_0 \exp(-2r^2/W_p^2)\,. \quad (11)$$

However, if squares and higher powers of $(2r^2/W_p^2)$ are ignored in the expansion of (11), it follows that close to the z axis where the fields are strongest, G has a parabolic radial dependence. The Raman cell then appears like the generalised lens-like medium considered by Kogelnik [9], and the resulting wave equation has exact solutions. We use this approach to make useful first-order calculations, and the results obtained by approximating the gain profile in this way are justified later by comparing with the results of a numerical analysis for an exact Gaussian profile.

To simplify the explanation at first, we take a constant $1/e$ pump field radius W_p throughout the medium. Then assuming circular cylindrical symmetry for the Stokes beam, (8) becomes

$$\frac{1}{r}\frac{\partial}{\partial r}\left(r\frac{\partial E_s}{\partial r}\right)-2jk_s\frac{\partial E_s}{\partial z} +jk_sG_0(1-2r^2/W_p^2)E_s=0\,. \tag{12}$$

Exact solutions of (12) are the Gaussian-Laguerre modes, of which the lowest order is the Gaussian wave

$$E_s=A\exp\left[-j(\phi+\tfrac{1}{2}Qr^2)\right], \tag{13}$$

where the amplitude A and phase ϕ are real functions of distance z, and Q is related to the Stokes complex beam parameter q [20] by

$$Q/k_s=1/q=1/R_s-2j/k_sW_s^2\,. \tag{14}$$

W_s is the $1/e$ field radius, and the radius of curvature R_s is positive for a beam whose wavefront is convex in the direction of propagation.

Substituting (13) in (12) and separating the terms with equal powers of r gives the pair of equations

$$Q^2/k_s+dQ/dz+j2G_0/W_p^2=0 \tag{15}$$

and

$$jQ/k_s+(j/A)dA/dz+d\phi/dz-jG_0/2=0\,. \tag{16}$$

Kogelnik [9] has shown that there is a *matched* Gaussian mode Q_m whose beam parameters remain constant whilst propagating through the medium. Postulating $dQ_m/dz=0$, (15) gives

$$Q_m^2=-j2k_sG_0/W_p^2\,. \tag{17}$$

Selecting the root which gives a real and positive spot size, and separating the real and imaginary parts gives

$$R_{sm}=(k_sW_p^2/G_0)^{\frac{1}{2}} \tag{18}$$

and

$$W_{sm}^2=2(W_p^2/G_0k_s)^{\frac{1}{2}} \tag{19}$$

for the matched values of the radius of curvature and spot size.

The development of a Stokes beam having an initial beam parameter Q_1 as it propagates through the Raman active medium is obtained from the propagation Eq. (15). For the matched beam $(Q_1=Q_m)$, the beam parameter Q is stationary throughout the medium, but if the input beam is not matched, then the beam diameter and radius of curvature fluctuate with distance z, tending towards the matched values [Ref. 9, Eq. (34)]. From this equation, it follows that for any initial value Q_1, Q converges with the matched value Q_m after a distance of about $3R_{sm}$.

The imaginary part of (16) gives the result

$$(1/A)\,dA/dz=G_0/2-1/R_s \tag{20}$$

which shows the relationship between the Stokes field amplitude and the parameters of the pump and Stokes beams. The final term in (20) represents the reduction in amplitude which results from the diffraction spread of a Gaussian beam. The net increase in the amplitude of the Stokes field over a length L is obtained by integrating (20), and for a matched beam $(Q=Q_m)$ for which R_s is constant, the result is

$$A(L)/A(0)=\exp[(\tilde{P}_p-2\sqrt{\tilde{P}_p})\,L/2k_sW_p^2]\,, \tag{21}$$

where we have introduced the expression

$$\tilde{P}_p=G_0k_sW_p^2\,. \tag{22}$$

From (9) and (11), it may be seen that $\tilde{P}_p$ is a dimensionless quantity related to the incident pump power P_p,

$$\tilde{P}_p=4\mu_0\chi_R\omega_p\omega_s^2\,P_p/\pi k_pc^2\,. \tag{23}$$

In a gas or vapour where refractive indices are almost unity,

$$\tilde{P}_p=4\mu_0\chi_R\kappa^2\omega_p^2P_p/\pi c \tag{24}$$

where $\kappa=k_s/k_p$. Equation (21) shows that there is an overall gain for the matched mode only if the pump power $\tilde{P}_p>4$. If $\tilde{P}_p$ is less than this, then the loss due to diffraction spread exceeds the gain which the Stokes wave receives from the scattering process. This represents a fundamental *gain threshold*, which differs from the usual experimental threshold criterion referring to the point at which the Stokes wave has built up to a detectable level (*detector threshold*). This will be discussed more fully later.

In order to justify these results obtained by using a parabolic approximation to the gain profile, we also obtained numerical solutions in the case of a Gaussian profile. Equations (8) and (9) are recast in dimensionless form, and the corresponding finite difference equations are solved using a computer [19]. Figures 2 and 3 show typical results for Stokes wave propagation in a medium with a constant pump

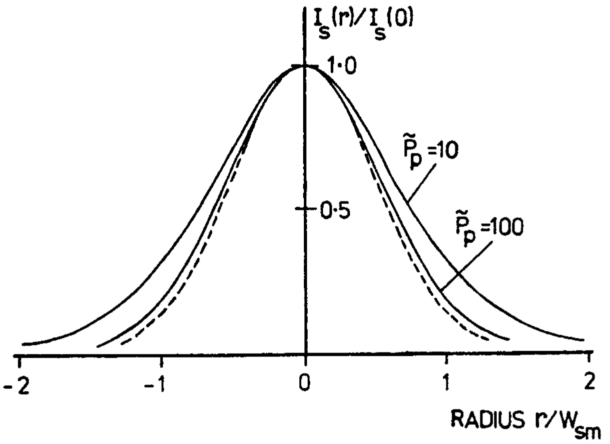

Fig. 2. Matched Stokes intensity profiles are shown for two values of the normalised pump power $\tilde{P}_p$. The computer results (solid lines) are compared with the Gaussian profile $\exp(-2r^2/W_{sm}^2)$ (broken line)

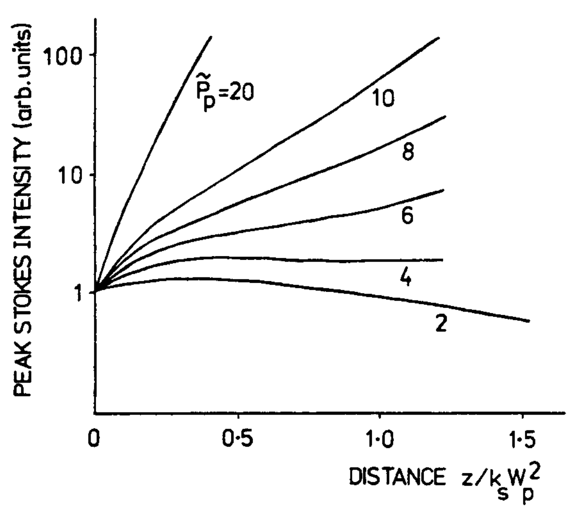

Fig. 3. Computer results showing the growth of the peak intensity of matched Stokes beams (for various values of normalised pump power $\tilde{P}_p$) as they propagate through the Raman medium

beam radius. Figure 2 exhibits the field distributions that were obtained for steady state (matched) Stokes modes, and demonstrates that even with pump powers close to the gain threshold, the Stokes fields are almost Gaussian with a $1/e$ radius of $\sim W_{sm}$. Figure 3 illustrates the growth in peak intensity of Stokes light beams that were matched at the input of the medium, and indicates that growth occurs when the normalised pump power $\tilde{P}_p$ is greater than about 4, whilst for values of $\tilde{P}_p$ less than this, the intensity actually falls. These results appear to justify the simple analytical approach.

The theory can be extended to cover the case which is of practical interest, in which an incident TEM_{00} mode pump beam, with confocal parameter b_p, is focussed to a waist W_{po} at a distance z_f inside the medium. The pump field $1/e$ radius is given by

$$W_p = W_{po}(1+\xi^2)^{\frac{1}{2}}\,, \tag{25}$$

where $\xi = 2(z-z_f)/b_p$.

The earlier analysis can be repeated with the addition that W_p can vary in the z direction, to give equations similar to (15) and (20),

$$Q(z)^2/k_s + dQ(z)/dz + j2\tilde{P}_p/k_s W_p(z)^4 = 0 \tag{26}$$

and

$$[1/A(z)]\,dA(z)/dz = \tilde{P}_p/2k_s W_p(z)^2 - 1/R_s(z) \tag{27}$$

noting that in this small signal analysis, the pump power $\tilde{P}_p$ remains constant. In this case, one can again define a matched beam parameter $Q_m(z)$, but in a more general sense than before; an input beam not having the matched parameter will tend to the matched beam as it propagates through the medium. A very good approximation to this matched parameter for a generated Stokes beam is given by

$$Q_m = [2\kappa\xi + (1-j)\sqrt{\tilde{P}_p}]/W_{po}^2(1+\xi^2)\,. \tag{28}$$

Then, as before, one may integrate (27) to find the increase in the matched Stokes field over the cell length L, and if, as is usual, the pump beam is focussed at the centre of the cell ($z_f = \frac{1}{2}L$), then the result obtained is

$$A(L)/A(0) = \exp\{[(\tilde{P}_p - 2\sqrt{\tilde{P}_p})/2\kappa]\,\arctan(L/b_p)\}\,. \tag{29}$$

We now apply these results to single pass Raman generation, in which one pass through the scattering cell is sufficient to amplify the spontaneous Stokes signal to a detectable level. For generating radiation which can be tuned in frequency, one wants to be able to predict the pump power P_{pth} which would be required to reach *detector threshold* (i.e. to generate some minimum detectable Stokes power $P_s(L)_{th}$) at a particular wavelength. Alternatively, for a given available pump power, one may wish to calculate the tuning range over which the generated power will exceed the detectable minimum. For a given value of the Raman susceptibility χ_R, the threshold pump power [Watts] calculated from (24) and (29) is

$$P_{\text{pth}} = \frac{\pi c[1+\{1+[\kappa/\arctan(L/b_p)]\ln[P_s(L)_{\text{th}}/P_{so}]\}^{\frac{1}{2}}]^2}{4\mu_0 \chi_R \kappa^2 \omega_p^2}, \quad (30)$$

where P_{so} is the spontaneous Raman power coupled into the matched Stokes mode. This equation shows that to minimise the threshold, the pump beam should be strongly focussed in the cell (large value for L/b_p). In any particular case, the optimum focussing will depend on the breakdown and saturation characteristics of the medium. If the Raman shift is small ($\kappa \equiv k_s/k_p \sim 1$) then for typical threshold power gains of exp [30] and higher, (30) can be approximated by

$$P_{\text{pth}} = \frac{\pi c \ln[P_s(L)_{\text{th}}/P_{so}]}{4\mu_0 \chi_R \kappa \omega_p^2 \arctan(L/b_p)}. \quad (31)$$

Equation (31) is the result that would be obtained by ignoring gain focussing effects, and implies a $1/\kappa$ threshold power dependence. This would apply for example to Raman scattering of visible radiation in liquids. However, for generating infrared radiation using visible and near infrared pumping sources, κ is in the range 0.001–0.25 [3–8], and (30) predicts significantly increased threshold pump powers resulting from the infrared diffraction loss. For example, radiation at 20 µm has been produced using the $6s-10s$ electronic Raman transition in caesium vapour [5], and in that case ($\kappa=0.017$), taking $L/b_p=1$ typically, the necessary pump power predicted by the gain focussing analysis (30) is about 8 times greater than that estimated using (31). The difference between (30) and (31) becomes increasingly pronounced at longer generated wavelengths as (30) tends towards a $1/\kappa^2$ threshold dependence. For small κ, the *detector threshold* condition given by (30) tends to the condition $\tilde{P}_p=4$, which is the *gain threshold* condition given earlier. This illustrates that diffraction loss is the dominant factor in determining the threshold for long wavelength generation.

Finally in this section, we briefly consider the effect of the real part of the Raman susceptibility, which represents a contribution to the Stokes refractive index which is proportional to the intensity of the incident pump radiation (optical Kerr effect). This gives rise to a pump-induced focussing or defocussing of the Stokes light, and has recently been observed experimentally on a Raman transition in benzene [21]. Taking as an example homogeneous (Lorentzian) dispersion of the Raman susceptibility, then

$$\chi^{(3)}(-\omega_s; \omega_p, -\omega_p, \omega_s) = \chi_R/(\tilde{\omega}_s - j), \quad (32)$$

where $\tilde{\omega}_s = 2(\omega_s + \omega_{gf} - \omega_p)/\Gamma$, Γ is the spontaneous Raman linewidth (FWHM), and χ_R is real as before. On the high frequency side of the Raman transition ($\tilde{\omega}_s > 0$), there is an increase in the Stokes refractive index at the centre of the beam where the incident radiation is strongest. This tends to reduce the divergence of the Stokes wavefront, and so lowers the diffraction loss. There is a corresponding increase in divergence on the low frequency side ($\tilde{\omega}_s < 0$). One therefore expects the net Stokes gain to be greatest at some frequency displaced to the high frequency side of the exact resonance given in (5). This is very similar to the frequency pulling effect which can occur in gas lasers due to the real part of the susceptibility associated with the laser transition (dispersion focussing) [14]. Repeating the previous analysis, but including the contribution due to the real part of $\chi^{(3)}$, Eq. (29) now becomes

$$A(L)/A(0) = \exp\left\{\left[\frac{\tilde{P}_p}{1+\tilde{\omega}_s^2} - 2\left(\frac{\tilde{P}_p((1+\tilde{\omega}_s^2)^{\frac{1}{2}} - \tilde{\omega}_s)}{1+\tilde{\omega}_s^2}\right)^{\frac{1}{2}}\right] \arctan(L/b_p)/2\kappa\right\}. \quad (33)$$

A similar expression can be derived for a Doppler broadened Raman transition [14]. Fig. 4 shows the Stokes gain given by (33) plotted as a function of frequency $\tilde{\omega}_s$ for various values of the normalised pump power $\tilde{P}_p$. The frequency for maximum gain shifts increasingly to the high frequency side of the transition as $\tilde{P}_p$ is reduced. Eventually the gain threshold (the point at which the diffraction loss exactly equals the gain) is reached when $\tilde{P}_p = 3.08$, at the frequency $\tilde{\omega}_s = 0.58$. (Previously when we neglected dispersion focussing, the gain threshold was $\tilde{P}_p = 4$).

These results indicate that as the pump power is reduced towards the gain threshold, there is an increasing frequency pulling effect which can result in the generated radiation being shifted by as much as a quarter of the full-width spontaneous Raman linewidth. As already pointed out, for longer wavelengths there is a decreasing margin between the *detector threshold* and the *gain threshold*, and so the frequency shift of the output becomes increasingly severe. To take an example, for generating 3.0 μm radiation using the 4*s*–5*s* electronic Raman transition in potassium vapour ($\kappa = 0.137$) [7], the pump power required to reach exp [30] Stokes power gain, calculated from (33) assuming $L = b_p$, is $\tilde{P}_p = 11.8$. The corresponding shift would be $\tilde{\omega}_s = 0.19$ shown as point *a* on Fig. 4. A second example at a longer wavelength is that of 20 μm generation using the 6s–10s transition in caesium vapour ($\kappa = 0.017$) [5]. Taking the same experimental conditions as in the previous example, the detector threshold calculated from (33) is $\tilde{P}_p = 4.6$, and the frequency shift is $\tilde{\omega}_s = 0.38$, indicated by point *b* on Fig. 4. If the pump power is now increased above the detector threshold, then the frequency shift will be reduced. Provided our small signal analysis is not violated, Fig. 4 indicates that in the second example given above, an increase in pump power by a factor of 2 above the detector threshold will decrease the frequency shift from $\tilde{\omega}_s = 0.38$ (point *b*) to $\tilde{\omega}_s = \sim 0.22$ (point *c*). This means that a variation in power during the incident pump pulse can result in a corresponding rapid variation (chirp) in the Stokes frequency. These examples illustrate the way in which gain and dispersion focussing can limit the ultimate frequency purity of the generated radiation.

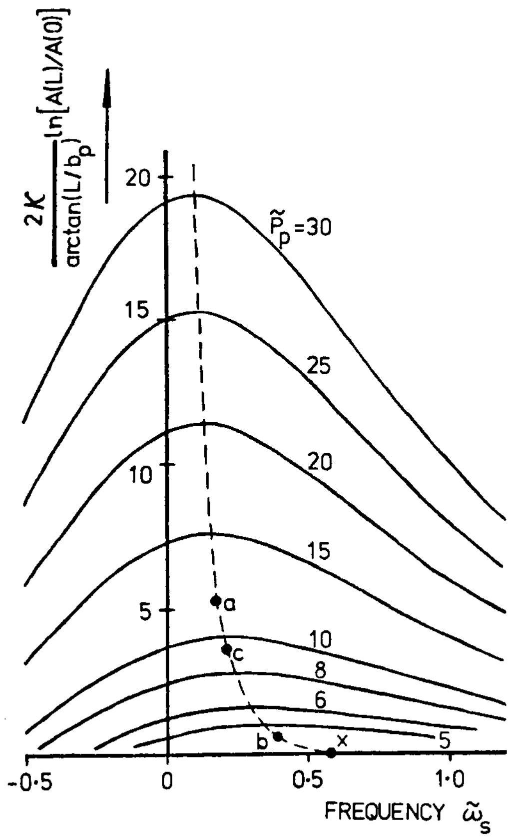

Fig. 4. Stokes gain spectra are shown for different values of normalised pump power $\tilde{P}_p$. As the pump power is reduced, the frequency for maximum gain (broken line) shifts increasingly to the high frequency side. The gain threshold (point *x*) is reached when $\tilde{P}_p = 3.08$, at $\tilde{\omega}_s = 0.58$

2. Raman Oscillator

It is well known that the modes obtained in high gain lasers may depart appreciably from those predicted by empty resonator theory [20], and this has been successfully explained in certain cases by taking into account the spatial variations of gain and refractive index found in such lasers [10–13]. Recently a number of papers have been devoted to extending Kogelnik's analysis of propagation in lens-like media [9] to predict the modes and stability of optical resonators in which gain focussing mechanisms are present [10–16]. In the same way, the Raman gain focussing analysis developed here can be used to investigate the behaviour of a Raman oscillator. The oscillator is assumed to consist of a scattering cell between a pair of mirrors which partially reflect the Stokes light whilst wholly transmitting the pump light [1]. Repeated reflection of the Stokes wave increases the overall amplification and hence the available tuning range. We show here however that for infrared generation it is important to take diffraction effects into account when making theoretical predictions of threshold.

It is assumed in what follows that the oscillator mode is wholly confined (the dimensions of the beams remain finite inside the cavity) [15], and so may be completely described within the limits of Gaussian beam theory. It is then possible to integrate (27) to calculate the round-trip gain experienced by the Stokes wave. Hence the resonator can only sustain continuous (cw) oscillations if

$$(\tilde{P}_p/k_s)\int_0^L dz/W_p^2 \geq \oint dz/R_s - \ln r\,, \tag{34}$$

where L is the distance between the mirrors, r is the average field reflectivity at the Stokes wavelength, and from (23), $\tilde{P}_p$ is zero outside the Raman medium ($\chi_R=0$). It has been assumed in (34) that the gain coefficients for the forward and backward travelling Stokes waves are equal, although there is an obvious extension in cases where this is not true [22]. The loop integration on the right hand side of (34) is carried out over a complete round trip of the cavity using the sign convention for R_s defined earlier. This integral, which is non-zero in the presence of gain focussing and represents the diffraction loss from the generated radiation, can substantially increase the oscillation threshold. If the threshold condition is not satisfied, the amplitude reduction due to losses and diffraction spread exceeds the gain which the beam receives from the scattering process, and the resonator is incapable of sustaining oscillations. For pulsed operation, the overall Stokes amplification must be sufficient for the Stokes wave to reach some minimum detectable level within the duration of the pumping pulse, and for a threshold power gain of 10^n per round trip,

$$(\tilde{P}_p/k_s)\int_0^L dz/W_p^2 \geq (n/2)\ln 10 + \oint dz/R_s - \ln r\,. \tag{35}$$

In a low-loss cavity, the cw oscillation threshold will be close to the gain threshold described in Section 1. In that case, and for small Raman shifts ($\kappa \simeq 1$), our result (34) agrees closely with that of an analysis in which gain focussing effects are neglected [23]. However, for infrared generation the results obtained using (34) and (35) differ considerably.

To evaluate (34) and (35) it is first necessary to know R_s, the radius of curvature of the Stokes wavefront, throughout the cavity. For any particular case, the propagation equation (26) together with the appropriate beam transformations corresponding to reflection at the mirrors can be solved numerically to find the self-consistent Gaussian mode of the resonator. Following this procedure, the threshold pump power can be calculated and optimised with respect to the parameters of the medium, mirrors and pump beam focussing.

By way of illustration we consider a particularly simple example (not requiring computer analysis) of a plane parallel resonator in which the incident pump beam spot size W_p is assumed constant throughout the medium. Also we assume that the scattering cell fills the space between the mirrors. By considering the unfolded resonator it can be seen that this corresponds to a uniform lens-like medium of infinite extent. From Kogelnik's analysis [9] it then follows that the Stokes light is simply confined in the matched mode Q_m given by (17). (Although this resonator is unstable in the conventional sense [20], the focussing due to the Raman gain profile results in stable confined modes of oscillation [15].) Integrating (35) in this case gives the detector threshold criterion

$$L[\tilde{P}_p - 2(\tilde{P}_p)^{\frac{1}{2}}]/\kappa b_p \geq (n/2)\ln 10 - \ln r\,, \tag{36}$$

where $\kappa = k_s/k_p$, and our assumption of constant pump beam spot size implies that the confocal parameter $b_p \gtrsim L$. The square root term on the left-hand side of (36) represents the additional loss due to diffraction of the generated wave. The effect of this loss can be demonstrated by comparing the threshold calculated from (36) with the detector threshold for single-pass generation in a cell of the same length. In both cases we will take a pump beam confocal parameter b_p equal to twice the cell length, and so our assumption of constant pump spot size is reasonable. We will also assume that a threshold power gain of exp [30] is required, and take the following typical oscillator parameters; $r=0.95$ (representing $\sim 90\%$ Stokes intensity reflectivity for the output coupling mirror), $n=0.5$ (implying ~ 26 round trips necessary to reach threshold). For Raman oscillation on the first Stokes line in hydrogen gas using a pump wavelength of 580 nm ($\kappa=0.76$) [1], the threshold calculated from (36) is $\tilde{P}_p=5.8$. Whereas the corresponding detector threshold for single-pass generation calculated from (29) is $\tilde{P}_p=61$, and so in this case an oscillator configuration can reduce the threshold pump power by about an order of magnitude [1]. However, for Raman oscillation at 20 μm using the 6s–10s electronic Raman transition in caesium ($\kappa=0.017$) [5], the situation is quite different. In that case the threshold calculated from (36) is $\tilde{P}_p=4.05$, whereas the single pass generation threshold from (29) is $\tilde{P}_p=5.9$, representing a reduction of only some 30% by using an oscillator.

These examples have been given simply to illustrate that our analysis suggests that, because of the limits imposed by the diffraction loss particularly at longer wavelengths, an oscillator configuration does not necessarily result in a substantial reduction in the threshold pump power (and corresponding increase in tuning range) when compared with single-pass generation. However, there are some situations where an oscillator could be of value, even for long wave generation. For example, if a very high pump power is available, it may be necessary to use a large pump beam spot size W_p in the medium. This can imply either that a very long cell should be used (thus keeping $L/b_p \simeq 1$), or it may prove more convenient to use a short cell in an oscillator configuration.

In order to clarify the explanation, throughout this section we have ignored the effect of the induced focussing which arises from the real part of the Raman susceptibility. However, following the outline given in Section 1, the theory can be extended to take this into account. In the example we have considered, a plane parallel resonator with weak pump beam focussing, the frequency dependence of the single pass gain will be that shown in Fig. 4. For a given pump power $\tilde{P}_p$, the longitudinal mode which is nearest in frequency to the maximum on the gain curve will be the one which oscillates [14].

Conclusions

The theory of gain focussing has been used to analyse the growth and propagation of stimulated Raman radiation. It has been found that for long wavelength generation, diffraction effects can become dominant, and lead to a considerable decrease in the effective gain. This raises the threshold and reduces the available tuning range. Frequency pulling due to the dispersion of the Raman susceptibility has also been analysed, and under some conditions can be a significant fraction of the spontaneous Raman linewidth. Finally, it has been found that an oscillator configuration will not necessarily produce a dramatic reduction in threshold.

Acknowledgements. We wish to thank Professor M. Maier for helpful discussions, and for providing details of the computer calculations used in [19]. This work has been supported by the U.K.A.E.A. Culham Laboratory. D. Cotter and R. Wyatt hold Science Research Council Studentships.

References

1. W. Schmidt, W. Apt: Z. Naturforsch. **27**A, 1373 (1972)
   W. Schmidt, W. Apt: IEEE J. Quant. Electr. **QE-10**, 792 (1974)
2. R. Frey, F. Pradere: Opt. Commun. **12**, 98 (1974)
3. M. Rokni, S. Yatsiv: Phys. Letters **24A**, 277 (1967)
4. P. P. Sorokin, N. S. Shiren, J. R. Lankard, E. C. Hammond, T. G. Zazyaka: Appl. Phys. Letters **10**, 44 (1967)
5. P. P. Sorokin, J. R. Lankard: IEEE J. Quant. Electr. **QE-9**, 227 (1973)
6. J. L. Carlsten, P. C. Dunn: Opt. Commun. **14**, 8 (1975)
7. D. Cotter, D. C. Hanna, P. A. Karkkainen, R. Wyatt: Opt. Commun. (1975), to be published
8. J. J. Wynne, P. P. Sorokin: J. Phys. B (Atom. Molec. Phys.) **8**, L37 (1975)
9. H. Kogelnik: Appl. Opt. **4**, 1562 (1965)
10. L. Casperson, A. Yariv: Appl. Phys. Letters **12**, 355 (1968)
11. L. Casperson, A. Yariv: Appl. Opt. **11**, 462 (1972)
12. G. J. Ernst, W. J. Witteman: IEEE J. Quant. Electr. **QE-9**, 911 (1973)
13. W. J. Witteman, G. J. Ernst: Appl. Phys. **6**, 297 (1975)
14. G. J. Ernst, W. J. Witteman: IEEE J. Quant. Electr. **QE-10**, 37 (1974)
15. L. W. Casperson: IEEE J. Quant. Electr. **QE-10**, 629 (1974)
16. U. Ganiel, Y. Silberberg: Appl. Opt. **14**, 306 (1975)
17. J. Ducuing: *Proc. Intern. School of Physics Enrico Fermi, Course XLII, Quantum Optics*, Ed. by R. J. Glauber, (Academic Press, New York, London 1969) pp. 421–472
18. M. Lax, M. H. Louisell, W. B. McKnight: Phys. Rev. A**11**, 1365 (1975)
19. O. Rahn, M. Maier: Phys. Rev. A**9**, 1427 (1974)
20. H. Kogelnik, T. Li: Appl. Opt. **5**, 1550 (1966)
21. A. Owyoung: Appl. Phys. Letters **26**, 168 (1975)
22. I. M. Beterov, Yu. A. Matyugin, V. P. Chebotaev: Sov. Phys. JETP **37**, 756 (1973)
23. G. D. Boyd, W. D. Johnston, I. P. Kaminow: IEEE J. Quant. Electr. **QE-5**, 203 (1969)